Inorg. Chem. **2002**, *41*, 3533–3541

Synthesis and Characterization of Mononuclear Zinc Aryloxide Complexes Supported by Nitrogen/Sulfur Ligands Possessing an Internal Hydrogen Bond Donor

Dewain K. Garner,[†] Russell A. Allred,[†] Kyle J. Tubbs,[†] Atta M. Arif,[‡] and Lisa M. Berreau*[,†]

Department of Chemistry and Biochemistry, Utah State University, Logan, Utah 84322-0300, and Department of Chemistry, University of Utah, Salt Lake City, Utah 84112

Received January 10, 2002

Treatment of a dinuclear zinc hydroxide complex ([(bmnpaZn)$_2$(μ-OH)$_2$](ClO$_4$)$_2$ (**1**) or [(benpaZn)$_2$(μ-OH)$_2$](ClO$_4$)$_2$ (**2**)) with excess equivalents of an aryl alcohol derivative (*p*-HOC$_6$H$_4$X; X = NO$_2$, CHO, CN, COCH$_3$, Br, H, OCH$_3$) yielded the nitrogen/sulfur-ligated zinc aryloxide complexes [(bmnpa)Zn(*p*-OC$_6$H$_4$NO$_2$)](ClO$_4$) (**3**), [(benpa)Zn(*p*-OC$_6$H$_4$NO$_2$)](ClO$_4$) (**4**), [(benpa)Zn(*p*-OC$_6$H$_4$CHO)](ClO$_4$) (**5**), [(benpa)Zn(*p*-OC$_6$H$_4$CN)](ClO$_4$) (**6**), [(benpa)Zn(*p*-OC$_6$H$_4$-COCH$_3$)](ClO$_4$)·0.5H$_2$O (**7**), [(benpa)Zn(*p*-OC$_6$H$_4$Br)](ClO$_4$) (**8**), [(benpa)Zn(*p*-OC$_6$H$_5$)](ClO$_4$) (**9**), and [(benpa)Zn(*p*-OC$_6$H$_5$OCH$_3$)](ClO$_4$) (**10**). The solid state structures of **2**, **3**, **5**, and **6** have been determined by X-ray crystallography. While **3** and **6** exhibit a mononuclear zinc ion possessing a distorted five-coordinate trigonal bipyramidal geometry, in **5** each zinc center exhibits a distorted six-coordinate octahedral geometry resulting from coordination of the aldehyde carbonyl oxygen of another zinc-bound aryloxide ligand, yielding a chain-type structure. Zinc coordination of the aldehyde carbonyl of **5** is indicated by a large shift (>40 cm^{-1}) to lower energy of the carbonyl stretching vibration ($\nu_{C=O}$) in solid state FTIR spectra of the complex. In the solid state structures of **3**, **5**, and **6**, a hydrogen-bonding interaction is found between N(3)–H of the supporting bmnpa/benpa ligand and the zinc-bound oxygen atom of the aryloxide ligand (N(3)···O(1) $\sim$ 2.78 Å). Solution ^{1}H and ^{13}C NMR spectra of **3**–**10** in CD$_3$CN and FTIR spectra in CH$_3$CN are consistent with all of the aryloxide complexes having a similar solution structure, with retention of the hydrogen-bonding interaction involving N(3)–H and the oxygen atom of the zinc-coordinated aryloxide ligand. For this family of zinc aryloxide complexes, a correlation was discovered between the chemical shift position of the N(3)–*H* proton resonance and the pK_a of the parent aryl alcohol. This correlation indicates that the strength of the hydrogen-bonding interaction involving the zinc-bound aryloxide oxygen is increasing as the aryloxide moiety increases in basicity.

Introduction

The zinc-containing enzyme liver alcohol dehydrogenase (LADH) catalyzes the two-electron oxidation of an alcohol to an aldehyde or ketone, coupled with reduction of NAD$^+$ to NADH.[1] In the resting state, the tetrahedral ligand environment of the active site zinc ion in LADH is composed of a histidine nitrogen donor, two cysteine thiolate sulfur donors, and a water/hydroxo moiety. During catalytic turnover, it is proposed the zinc-bound alcohol substrate undergoes deprotonation to yield a zinc-bound alkoxide species, which is suggested to be the active complex for hydride transfer to NAD$^+$.[2] An active site residue that interacts with the zinc-bound alkoxide is Ser$_{48}$. As shown in Scheme 1, this residue is proposed to donate a hydrogen bond to the oxygen atom of the zinc-bound alkoxide.[2] Structural or spectroscopic parameters for this Ser$_{48}$ hydrogen-bonding interaction involving a zinc−alkoxide species in LADH have not been reported.[3] However, structurally characterized forms of LADH inhibited by formamides[4] or sulfoxides[5] exhibit a

* Corresponding author. E-mail: berreau@cc.usu.edu. Phone: (435) 797-1625. Fax: (435) 797-3390.
† Utah State University.
‡ University of Utah.

(1) Eklund, H.; Brändén, C.-I. In *Zinc Enzymes*; Spiro, T. G., Ed.; Wiley: New York, 1983; pp 124−152.

(2) Ramaswamy, S.; Park, D.-H.; Plapp, B. V. *Biochemistry* **1999**, *38*, 13951−13959.

(3) A calculated O(Ser$_{48}$)···O(alkoxide) distance (2.44 Å) was recently reported. Agarwal, P. K.; Webb, S. P.; Hammes-Schiffer, S. *J. Am. Chem. Soc.* **2000**, *122*, 4803−4812.

10.1021/ic020031q CCC: $22.00
Published on Web 06/07/2002

Scheme 1. Hydrogen-Bonding Interactions in LADH Involving Ser_{48}

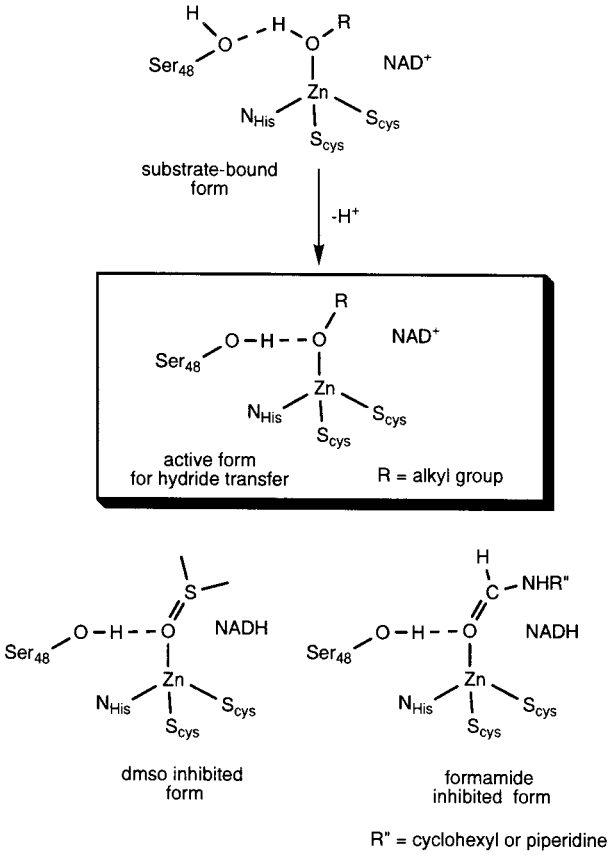

hydrogen-bonding interaction between Ser_{48} (H-bond donor) and the zinc-bound oxygen atom of the inhibitor (H-bond acceptor) that is likely similar to that involving the zinc-bound alkoxide. The hydrogen-bonding interactions found in these inhibited forms of LADH are characterized by short heteroatom distances ($O(Ser_{48})\cdots O(inhibitor)$, ~2.6 Å).[6]

Despite the synthesis of zinc complexes of several new mixed nitrogen/sulfur ligand systems in recent years,[7−10] synthetic zinc alkoxide or aryloxide complexes possessing a mixed nitrogen/sulfur coordination environment remain elusive synthetic targets.[11,12] This is likely due in part to the dearth of known nitrogen/sulfur-ligated zinc hydroxide species,[13] molecules that may serve as synthetic precursors to alkoxide/aryloxide derivatives.

In our laboratory, we have developed a family of nitrogen/sulfur(thioether) ligands possessing a single internal hydrogen bond donor. While these ligands possess neutral sulfur donors, versus the anionic cysteine sulfur donors found in LADH, they have proven suitable for isolating several complexes relevant to this enzyme. Specifically, by using thioether sulfur donors in our ligands, we can prevent the formation of thiolate bridged polymetallic complexes,[14] and hence produce zinc complexes with available coordination sites for binding of small molecules relevant to substrate or inhibitors. For example, using the bmapa ligand (*N*,*N*-bis-2-(methylthio)ethyl-*N*-(6-amino-2-pyridylmethyl)amine), we recently prepared and structurally characterized mononuclear zinc alcohol and formamide complexes relevant to substrate and inhibitor-bound forms of LADH.[15] Importantly, the *N*,*N*-dimethylformamide complex exhibits a secondary hydrogen-bonding interaction akin to that involving Ser_{48} in the formamide-inhibited form of LADH.[4]

We have also demonstrated that another member of this ligand family (*N*,*N*-bis-2-(methylthio)ethyl-*N*-(6-neopentylamino-2-pyridylmethyl)amine, bmnpa) enables the isolation of a mononuclear nitrogen/sulfur-ligated zinc complex possessing a single bound anion (perchlorate).[13] This anion accepts a hydrogen bond from the secondary amine donor of the bmnpa ligand, thus providing an indication that the bmnpa ligand system may prove suitable for isolation of novel complexes possessing a single bound alkoxide or aryloxide ligand. Herein, we outline our initial exploration of the reactions of zinc hydroxide complexes of the bmnpa and benpa (*N*,*N*-bis-2-(ethylthio)ethyl-*N*-(6-neopentylamino-2-pyridylmethyl)amine) ligands with several aryl alcohols. Through this work, we demonstrate that these ligand sets enable the isolation and characterization of mononuclear nitrogen/sulfur-ligated zinc aryloxide complexes possessing a hydrogen-bonding interaction akin to that proposed to occur between Ser_{48} and a zinc-bound alkoxide in the active form of LADH. Furthermore, we outline how this hydrogen-bonding interaction is perturbed by changes in the basicity of the zinc-bound aryloxide ligand.

(4) Ramaswamy, S.; Scholze, M.; Plapp, B. V. *Biochemistry* **1997**, *36*, 3522−3527.
(5) Al-Karadaghi, S.; Cedergren-Zeppezauer, E.; Hövmoller, S.; Petratos, K.; Terry, H.; Wilson, K. S. *Acta Crystallogr.* **1994**, *D50*, 793−807.
(6) Jeffrey, G. A. *An Introduction to Hydrogen Bonding*; Oxford University Press: New York, 1997.
(7) For example, see: (a) Seebacher, J.; Shu, M. H.; Vahrenkamp, H. *Chem. Commun.* **2001**, 1026−1027 and references therein. (b) Burth, R.; Stange, A.; Schäfer, M.; Vahrenkamp, H. *Eur. J. Inorg. Chem.* **1998**, 1759−1764. (c) Brand, U.; Vahrenkamp, H. *Inorg. Chem.* **1995**, *34*, 3285−3293. (d) Brand, U.; Vahrenkamp, H. *Chem. Ber.* **1996**, *129*, 435−440.
(8) (a) Parkin, G. *Chem. Commun.* **2000**, 1971−1985. (b) Ghosh, P.; Parkin, G. *Chem. Commun.* **1998**, 413−414. (c) Kimblin, C.; Hascall, T.; Parkin, G. *Inorg. Chem.* **1997**, *36*, 5680−5681. (d) Kimblin, C.; Bridgewater, B. M.; Churchill, D. G.; Hascall, T.; Parkin, G. *Inorg. Chem.* **2000**, *39*, 4240−4243.
(9) (a) Chiou, S.-J.; Innocent, J.; Riordan, C. G.; Lam, K.-C.; Liable-Sands, L. M.; Rheingold, A. L. *Inorg. Chem.* **2000**, *39*, 4347−4353. (b) Chiou, S.-J.; Ge, P.; Riordan, C. G.; Liable-Sands, L. M.; Rheingold, A. L. *Chem. Commun.* **1999**, 159−160.
(10) (a) Chang, S.; Karambelkar, V. V.; diTargiani, R. C.; Goldberg, D. P. *Inorg. Chem.* **2001**, *40*, 194−195. (b) Shoner, S. C.; Humphreys, K. J.; Barnhart, D.; Kovacs, J. A. *Inorg. Chem.* **1995**, *34*, 5933−5934.
(11) Mononuclear zinc aryloxide/alkoxide complexes: (a) Tesmer, M.; Shu, M.; Vahrenkamp, H. *Inorg. Chem.* **2001**, *40*, 4022−4029. (b) Walz, R.; Weis, K.; Ruf, M.; Vahrenkamp, H. *Chem. Ber.* **1997**, *130*, 975−980. (c) Kimura, E.; Kodama, Y.; Koike, T.; Shiro, M. *J. Am. Chem. Soc.* **1995**, *117*, 8304−8311. (d) Kimura, E.; Nakamura, I.; Koike, T.; Shionoya, M.; Kodama, Y.; Ikeda, T.; Shiro, M. *J. Am. Chem. Soc.* **1994**, *116*, 4764−4771. (e) Bergquist, C.; Storrie, H.; Koutcher, L.; Bridgewater, B. M.; Friesner, R. A.; Parkin, G. *J. Am. Chem. Soc.* **2000**, *122*, 12651−12658. (f) Hammes, B. S.; Carrano, C. J. *Dalton Trans.* **2000**, 3304−3309.
(12) Mononuclear zinc alkoxide complexes ligated by tris(pyrazolyl)-hydroborato supporting ligands are known and have been studied as model systems for the active form of LADH: Bergquist, C.; Parkin, G. *Inorg. Chem.* **1999**, *38*, 422−423.
(13) Berreau, L. M.; Allred, R. A.; Makowska-Grzyska, M. M.; Arif, A. M. *Chem. Commun.* **2000**, 1423−1424.
(14) Burth, R.; Stange, A.; Schäfer, M.; Vahrenkamp, H. *Eur. J. Inorg. Chem.* **1998**, 1759−1764 and references cited therein.
(15) Berreau. L. M.; Makowska-Grzyska, M. M.; Arif, A. M. *Inorg. Chem.* **2001**, *40*, 2212−2213.

Experimental Section

All reagents and solvents were obtained from commercial sources and were used as received unless otherwise noted. Solvents were dried according to published procedures[16] and were distilled under N_2 prior to use. Synthetic reactions leading to the formation of the zinc aryloxide complexes were performed in a MBraun Unilab glovebox under an atmosphere of purified N_2. The ligand bmnpa and the dinuclear zinc hydroxide complex $[(bmnpaZn)_2(\mu\text{-}OH)_2](ClO_4)_2$ (**1**) were prepared as previously reported.[13]

Physical Methods. FTIR spectra were recorded on a Shimadzu FTIR-8400 spectrometer as KBr pellets or as CH_3CN or CH_2Cl_2 solutions (~100 mM) between NaCl plates. ^1H and $^{13}C\{^1H\}$ NMR spectra were recorded in dry CD_3CN at 20(1) °C on a JEOL GSX-270 or Bruker ARX400 spectrometer. Chemical shifts (in ppm) are referenced to the residual solvent peak(s) (^1H, 1.96 (quintet); $^{13}C\{^1H\}$, 1.39 (heptet) ppm). ^1H and ^{13}C NMR data for **2**−**10** may be found in Tables S3 and S4 of the Supporting Information. Elemental analyses were performed by Atlantic Microlabs of Norcross, GA.

CAUTION! *Perchlorate salts of metal complexes with organic ligands are potentially explosive. Only small amounts of material should be prepared, and these should be handled with great care.*[17]

***N,N*-Bis-2-(ethylthio)ethyl-*N*-(6-neopentylamino-2-pyridylmethyl)amine (benpa).** To a 500 mL round bottom flask was added 0.84 g (0.022 mol) $LiAlH_4$ followed by a solution of 35 mL of dry pyridine in 90 mL of dry THF. To this solution was added 2.6 g (0.0067 mol) of beppa (*N,N*-bis-2-(ethylthio)ethyl-*N*-(6-pivaloylamido-2-pyridylmethyl)amine)[18] dissolved in 85 mL of THF. The resulting solution was heated at reflux under a N_2 atmosphere for 14 h. After cooling the reaction mixture to ambient temperature, an equal volume of water was added, with the initial addition being done dropwise to minimize vigorous bubbling and emulsion formation. Extraction of the mixed organic/aqueous reaction mixture with EtOAc (3 × 100 mL), followed by drying of the combined organic fractions with Na_2SO_4, filtration, and removal of the solvent under reduced pressure, yielded a thick yellow oil. The analytically pure ligand (benpa) was isolated following column chromatography (ethyl acetate, 200−400 mesh silica gel, $R_f \sim 0.82$) as a yellow oil (73%). ^1H NMR (CD_3CN, 270 MHz): δ 7.32 (t, $J = 7.6$, 1H), 6.60 (d, $J = 7.2$, 1H), 6.33 (d, $J = 8.3$, 1H), 5.00 (t, $J = 5.6$ Hz, 1H, N−*H*), 3.56 (s, 2H), 3.13 (d, $J = 6.3$ Hz, 2H), 2.80−2.57 (m, 8H), 2.49 (q, $J = 7.2$ Hz, 4H), 1.18 (t, $J = 7.2$ Hz, 6H), 0.93 (s, 9H). $^{13}C\{^1H\}$ NMR (CD_3CN, 67.9 MHz): δ 160.2, 158.6, 138.2, 111.8, 106.3, 60.5, 55.1, 53.5, 32.9, 30.0, 27.9, 26.5, 15.4 (13 signals expected and observed). FTIR (neat, cm^{-1}): ~3400 (br, ν_{N-H}). Anal. Calcd for $C_{19}H_{35}N_3S_2$: C, 61.75; H, 9.55; N, 11.38. Found: C, 61.04; H, 9.62; N, 10.87.

$[(benpaZn)_2(\mu\text{-}OH)_2](ClO_4)_2$ (2). A methanol solution (1 mL) of benpa (0.10 g, 0.29 mmol) was added to methanol solution (2 mL) of $Zn(ClO_4)_2\cdot 6H_2O$ (0.10 g, 0.27 mmol). The resulting solution was stirred for ~30 min at ambient temperature, at which time a methanol solution (2 mL) of KOH (0.013 g, 0.28 mmol) was added. Following 30 min of rapid stirring, an excess of diethyl ether (15 mL) was added and the resulting cloudy mixture was cooled to ~ −28 °C for 30 min. A white solid that had deposited was then collected and dried briefly under vacuum. The solid precipitate obtained was then slurried in CH_3CN and was again added to excess Et_2O (20 mL). The precipitate obtained from this solution was taken up in CH_3CN (~10 mL), stirred vigorously for 20 min, and then filtered through a Celite/glass wool plug. Diethyl ether diffusion into this CH_3CN solution at ambient temperature yielded colorless crystalline blocks suitable for X-ray diffraction (0.13 g, 84%). The product was pure by ^1H NMR. FTIR (KBr, cm^{-1}): 3534 (ν_{O-H}), 3234 (ν_{N-H}), 1105 (ν_{ClO_4}), 624 (ν_{ClO_4}). Anal.Calcd for $C_{38}H_{72}N_6O_{10}S_4Cl_2Zn_2$: C, 41.52; H, 6.61; N, 7.65. Found: C, 40.02; H, 6.43; N, 7.37. Repeated attempts (three) at elemental analysis of this complex each time yielded a carbon content that is notably below the calculated value. We speculate that this may be due to the presence of trace amounts of $KClO_4$ that we have been unable to separate from the crystalline product. However, as shown below, aryloxide derivatives prepared from this zinc hydroxide complex are analytically pure.

General Method for the Preparation of $[(bmnpa)Zn(p\text{-}OC_6H_4X)]ClO_4$ and $[(benpa)Zn(p\text{-}OC_6H_4X)]ClO_4$ Complexes (bmnpa, X = NO_2 (3); benpa, X = NO_2 (4), CHO (5), CN (6), $COCH_3$ (7), Br (8), H (9), OCH_3 (10)). Part 1. In Situ Preparation of Zinc Hydroxide Complexes. Under atmospheric conditions, 0.11 g (0.29 mmol) of $Zn(ClO_4)_2\cdot 6H_2O$ was dissolved in methanol (2 mL). To this solution was added a pale yellow methanol solution (1 mL) of bmnpa (0.11 g, 0.31 mmol) or benpa (0.11 g, 0.28 mmol). The resulting mixture was stirred for 30 min at room temperature. At this point, a clear methanol solution of KOH (0.014 g, 0.30 mmol) was added and the solution was stirred for an additional 30 min. Excess Et_2O (~40 mL) was added, and the resulting cloudy solution was cooled to ~ −30 °C for 12 h. The solid that had deposited during this time was dried under vacuum. This solid was then dissolved in acetonitrile (5 mL), and an excess of Et_2O was added, leading to the rapid precipitation of a white solid, which was collected, dried under vacuum, and identified as either $[(bmnpaZn)_2(\mu\text{-}OH)_2](ClO_4)_2$ (**1**) or $[(benpaZn)_2(\mu\text{-}OH)_2](ClO_4)_2$ (**2**) by ^1H NMR spectroscopy.

Part 2. Reaction of Zinc Hydroxide Complexes with Aryl Alcohols. *Note: Dry solvents were employed throughout this procedure.* Under a dry, inert atmosphere, an acetonitrile (5 mL) solution of an excess (>4 equiv) molar amount of the desired phenol was added to 1 molar equiv of solid zinc hydroxide complex (**1** or **2**). The resulting slurry was stirred for 30 min, at which time the solvent was removed under reduced pressure. The dried solid was then dissolved in CH_2Cl_2 (5 mL) and filtered, and the filter cake was rinsed with several additional washes of methylene chloride (total volume ~10 mL). The volume of the filtrate solution was then reduced under vacuum to ~5 mL, excess Et_2O was added (~15 mL), and the resulting cloudy solution was cooled to ~ −20(1) °C for 12 h. The solid that had deposited was then dried under reduced pressure. Recrystallization of the product from diethyl ether diffusion into an acetonitrile solution containing an excess of the appropriate parent aryl alcohol (~0.015 g) yielded crystals suitable for X-ray diffraction analysis.

$[(bmnpa)Zn(p\text{-}OC_6H_4NO_2)]ClO_4$ (3). Yield: 137 mg, 73%. FTIR (KBr, cm^{-1}): 3220 (br, ν_{N-H}), 1299 (ν_{C-O}), 1086 (ν_{ClO_4}), 623 (ν_{ClO_4}). Anal. Calcd for $C_{23}H_{35}O_7N_4S_2ClZn$: C, 42.98; H, 5.49; N, 8.72. Found: C, 43.35; H, 5.57; N, 8.81.

$[(benpa)Zn(p\text{-}OC_6H_4NO_2)]ClO_4$ (4). Yield: 110 mg, 62%. FTIR (KBr, cm^{-1}): 3220 (br, ν_{N-H}), 1301 (ν_{C-O}), 1087 (ν_{ClO_4}), 622 (ν_{ClO_4}). Anal. Calcd for $C_{25}H_{39}O_7N_4S_2ClZn$: C, 44.77; H, 5.87; N, 8.36. Found: C, 44.46; H, 5.50; N, 8.39.

$[(benpa)Zn(p\text{-}OC_6H_4CHO)]ClO_4$ (5). Yield: 120 mg, 66%. FTIR (KBr, cm^{-1}): 3254 (br, ν_{N-H}), 1301 (ν_{C-O}), 1088 (ν_{ClO_4}), 623 (ν_{ClO_4}). FTIR (~100 mM CH_2Cl_2, cm^{-1}): 1685 ($\nu_{C=O}$). FTIR (~100 mM CH_3CN, cm^{-1}): 1680 ($\nu_{C=O}$). Anal. Calcd for

(16) Perrin, D. D.; Armarego, W. L. F. *Purification of Laboratory Chemicals*; Pergamon Press: New York, 1988.
(17) Wolsey, W. C. *J. Chem. Educ.* **1973**, *50*, A335−A337.
(18) Berreau, L. M.; Makowska-Grzyska, M. M.; Arif, A. M. *Inorg. Chem.* **2000**, *39*, 4390−4391.

$C_{26}H_{40}O_6N_3S_2ClZn$: C, 47.77; H, 6.17; N, 6.43. Found: C, 47.45; H, 6.18; N, 6.53.

[(benpa)Zn(*p*-OC$_6$H$_4$CN)]ClO$_4$ (6). Yield: 112 mg, 61%. FTIR (KBr, cm^{-1}): 3213 (ν_{N-H}), 2219 ($\nu_{C\equiv N}$), 1305 (ν_{C-O}), 1087 (ν_{ClO_4}), 622 (ν_{ClO_4}). Anal. Calcd for $C_{26}H_{39}O_5N_4S_2ClZn$: C, 47.99; H, 6.05; N, 8.62. Found: C, 47.89; H, 6.00; N, 8.54.

[(benpa)Zn(*p*-OC$_6$H$_4$COCH$_3$)]ClO$_4$·0.5H$_2$O (7). Yield: 112 mg, 59%. FTIR (KBr, cm^{-1}): 3246 (ν_{N-H}), 1648 ($\nu_{C=O}$), 1301 (ν_{C-O}), 1088 (ν_{ClO_4}), 623 (ν_{ClO_4}). FTIR (~100 mM CH_2Cl_2, cm^{-1}): 1662 ($\nu_{C=O}$). FTIR (~100 mM CH_3CN, cm^{-1}): 1662 ($\nu_{C=O}$). Anal. Calcd for $C_{27}H_{42}O_6N_3S_2ClZn\cdot0.5H_2O$: C, 47.92; H, 6.41; N, 6.21. Found: C, 47.77; H, 6.35; N, 6.30.

[(benpa)Zn(*p*-OC$_6$H$_4$Br)]ClO$_4$ (8). Yield: 129 mg, 66%. FTIR (KBr, cm^{-1}): 3209 (ν_{N-H}), 1279 (ν_{C-O}), 1091 (ν_{ClO_4}), 623 (ν_{ClO_4}). Anal. Calcd for $C_{25}H_{39}O_5N_3S_2ClBrZn$: C, 42.67; H, 5.59; N, 5.98. Found: C, 42.25; H, 5.34; N, 5.58.

[(benpa)Zn(OC$_6$H$_5$)]ClO$_4$ (9). Yield: 107 mg, 61%. FTIR (KBr, cm^{-1}): 3220 (ν_{N-H}), 1267 (ν_{C-O}), 1087 (ν_{ClO_4}), 623 (ν_{ClO_4}). Anal. Calcd for $C_{25}H_{40}O_5N_3S_2ClZn$: C, 47.99; H, 6.45; N, 6.72. Found: C, 47.66; H, 6.32; N, 6.50.

[(benpa)Zn(*p*-OC$_6$H$_5$OCH$_3$)]ClO$_4$ (10). Yield: 114 mg, 64%. FTIR (KBr, cm^{-1}): 3220 (ν_{N-H}), 1261 (ν_{C-O}), 1232 (ν_{C-O}), 1086 (ν_{ClO_4}), 623 (ν_{ClO_4}). Anal. Calcd for $C_{26}H_{42}O_6N_3S_2ClZn$: C, 47.62; H, 6.46; N, 6.41. Found: C, 48.04; H, 6.76; N, 6.11.

X-ray Crystallography. A crystal of each compound **2**, **3**, **5**, and **6** was mounted on a glass fiber with traces of viscous oil and then transferred to a Nonius KappaCCD diffractometer with Mo Kα radiation (λ = 0.71073 Å) for data collection at 200(1) K. For each compound, an initial set of cell constants was obtained from 10 frames of data that were collected with an oscillation range of 1 deg/frame and an exposure time of 20 s/frame. Indexing and unit cell refinement based on observed reflections from those 10 frames indicated monoclinic *P* lattices for **2**, **3**, **5**, and **6**. Final cell constants for each complex were determined from a set a strong reflections from the actual data collection. For each data set, these reflections were indexed, integrated, and corrected for Lorentz, polarization, and absorption effects using DENZO-SMN, SCALEPAC, and Multi-scan.[19] The structures were solved by a combination of direct methods and heavy atom using SIR 97. All of the non-hydrogen atoms were refined with anisotropic displacement coefficients. Unless otherwise stated, hydrogen atoms were assigned isotropic displacement coefficients U(H) = 1.2U(C) or 1.5U(C_{methyl}), and their coordinates were allowed to ride on their respective carbons using SHELXL97.

Structure Solution and Refinement. Crystals of **2** were determined to belong to the monoclinic crystal system. Systematic absences in the data for the zinc hydroxide complex [(benpaZn)$_2$(μ-OH)$_2$](ClO$_4$)$_2$ (**2**) were consistent with the space group $P2_1/n$. Hydrogen atoms were located and refined independently except those on C(5), C(5′), C(6), and C(6′), which were assigned isotropic displacement coefficients, and their coordinates were allowed to ride on their respective carbons. The carbon atoms of one thioether ethyl group of the benpa ligand exhibit disorder. These carbon atoms (C(5)/C(6)) were each split into two fragments (second fragment denoted by a prime) and were refined. This refinement led to a 0.48:0.52 ratio in occupancy over two positions for each carbon atom. The *p*-nitroaryloxide complex **3** crystallizes in the space group $P2_1/a$. Hydrogen atom H(3) was located and refined independently. The *p*-hydroxybenzaldehyde derivative **4** crystallizes in the space group $P2_1/n$. All hydrogen atoms were located and refined independently. The *p*-cyanoaryloxide complex **6** crystallizes in the space group $P2_1/a$. Hydrogen atoms were located and refined independently except those on C(5) and C(6), which were assigned isotropic displacement coefficients, and their coordinates were allowed to ride on their respective carbons.

(19) Otwinowski, Z.; Minor, W. *Methods Enzymol.* **1997**, *276*, 307−326.

Scheme 2

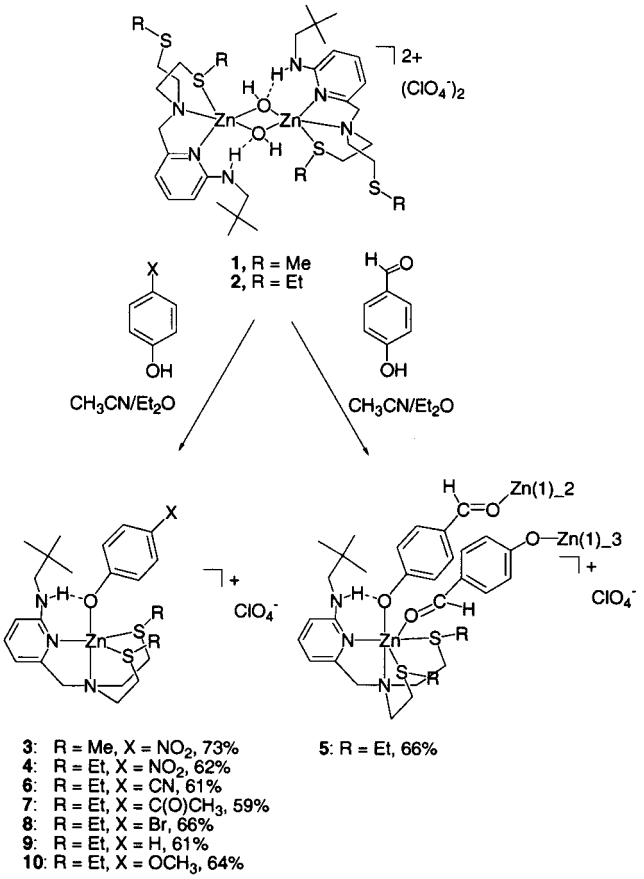

Results

Syntheses. Treatment of the dinuclear zinc hydroxide complexes [(bmnpaZn)$_2$(μ-OH)$_2$](ClO$_4$)$_2$ (**1**) or [(benpaZn)$_2$-(μ-OH)$_2$](ClO$_4$)$_2$ (**2**) with an excess (typically ~4 equiv) of an aryl alcohol derivative (*p*-HOC$_6$H$_4$X; X = NO$_2$, CHO, CN, COCH$_3$, H, Br, OCH$_3$; Scheme 2) yielded a series of nitrogen/sulfur-ligated zinc aryloxide complexes (**3**−**10**). The rationale for using excess equivalents of the aryl alcohol was the presence of trace amounts of [(benpaZn)$_2$(μ-OH)$_2$](ClO$_4$)$_2$ in isolated samples of some of the aryloxide complexes prepared under strictly stoichiometric conditions. Recrystallization of each complex from CH_3CN:Et_2O yielded an analytically pure crystalline material. Notably, the *p*-hydroxyacetophenone derivative **7** was consistently isolated with ~0.5 equiv of water present, even after prolonged drying under reduced pressure. Elemental analysis and ^{1}H NMR spectroscopy confirmed the presence of this water. In general, the aryloxide complexes are stable in dry CD_3CN solution for several days.

X-ray Crystallography. The structure of the zinc hydroxide derivative [(benpaZn)$_2$(μ-OH)$_2$](ClO$_4$)$_2$ (**2**) was determined by X-ray crystallography. Due to its nearly identical structural properties to the previously reported [(bmnpaZn)$_2$(μ-OH)$_2$](ClO$_4$)$_2$ (**1**), the metric features of this

Table 1. Details of X-ray Data Collection and Refinement for **3**, **5**, and **6**

	[(bmnpa)Zn(*p*-$OC_6H_4NO_2$)]ClO_4 (**3**)	[(benpa)Zn(*p*-OC_6H_4CHO)]ClO_4 (**5**)	[(benpa)Zn(*p*-OC_6H_4CN)]ClO_4 (**6**)
empirical formula	$C_{23}H_{35}ClN_4O_7S_2Zn$	$C_{26}H_{40}ClN_3O_6S_2Zn$	$C_{26}H_{39}ClN_4O_5S_2Zn$
fw	644.49	655.55	652.55
space group	$P2_1/a$	$P2_1/n$	$P2_1/a$
a, Å	15.8941(5)	13.0722(3)	15.2217(2)
b, Å	9.3054(2)	13.2501(3)	9.6944(2)
c, Å	19.8964	18.3831(4)	20.6876(4)
α, deg	90	90	90
β, deg	99.3345(12)	107.1365(9)	97.0568(7)
γ, deg	90	90	90
V, Å^3	2903.73(15)	3042.74(12)	3029.65(9)
Z	4	4	4
cryst color, habit	colorless thin plate	colorless prism	colorless plate
cryst size, mm^3	0.25 × 0.25 × 0.05	0.25 × 0.25 × 0.10	0.23 × 0.18 × 0.13
D(calcd), g cm^{-3}	1.474	1.431	1.431
μ(Mo Kα), mm^{-1}	1.129	1.075	1.078
temp, K	200(1)	200(1)	200(1)
diffractometer	Nonius KappaCCD	Nonius KappaCCD	Nonius KappaCCD
radiation	Mo Kα (0.71073 Å)	Mo Kα (0.71073 Å)	Mo Kα (0.71073 Å)
reflns collcd	12116	11638	11950
indep reflns	6623	6921	6925
params	352	512	489
R(*F*), %[a]	4.67	4.42	4.76
R(wF^2), %[a]	9.84	9.12	9.50
GOF on F^2 [b]	1.027	1.042	1.022
min and max resid dens, e Å^{-3}	−0.646, 0.968	−0.467, 0.770	−0.562, 0.719

[a] $R(wF^2) = [\sum(wF_o^2 - F_c^2)/\sum(F_o^2)^2]^{1/2}$, $R = \sum(||F_o| - |F_c||)/\sum|F_o|$; for **3**, $w = 1/[\sigma^2(F_o^2) + (0.0429P)^2 + 2.1924P]$; for **5**, $w = 1/[\sigma^2(F_o^2) + (0.0441P)^2 + 0.4838P]$; and for **6**, $w = 1/[\sigma^2(F_o^2) + (0.0486P)^2 + 0.2698P]$, where $P = (F_o^2 + 2F_c^2)/3$. [b] Goodness of fit on $F^2 = [\sum(w(F_o^2 - F_c^2)/(n - p)]^{1/2}$, where *n* is the number of reflections and *p* is the number of parameters refined.

Table 2. Selected Bond Distances (Å) and Angles (deg)

	3	**5**	**6**
Zn(1)−O(1)	1.950(2)	1.962(2)	1.942(2)
Zn(1)−O(2)_2		2.2283(19)	
Zn(1)−S(1)	2.4766(8)	2.5801(8)	2.4483(8)
Zn(1)−S(2)	2.4529(9)	2.5760(8)	2.4853(9)
Zn(1)−N(1)	2.207(2)	2.212(2)	2.198(2)
Zn(1)−N(2)	2.068(2)	2.143(2)	2.096(2)
C(18)−O(1)	1.332(3)		
C(20)−O(1)		1.324(3)	1.336(4)
C(26)−O(2)		1.238(3)	
N(1)−Zn(1)−O(1)	178.49(9)	172.13(8)	175.60(9)
N(2)−Zn(1)−O(1)	99.99(9)	97.73(8)	98.21(9)
O(1)−Zn(1)−S(1)	95.51(7)	91.83(6)	100.10(7)
O(1)−Zn(1)−S(2)	96.51(7)	102.07(6)	94.81(8)
S(1)−Zn(1)−S(2)	113.15(3)	98.42(3)	108.27(3)
N(2)−Zn(1)−S(1)	130.54(7)	103.20(8)	116.29(7)
N(2)−Zn(1)−S(2)	111.30(7)	150.05(6)	130.15(7)
N(2)−Zn(1)−O(2)_2		81.91(8)	
O(2)_2−Zn(1)−S(1)		172.98(6)	
O(2)_2−Zn(1)−S(2)		75.12(5)	
N(1)−Zn(1)−N(2)	80.54(9)	79.42(8)	80.36(9)
N(1)−Zn(1)−S(1)	83.09(6)	81.76(6)	84.24(7)
N(1)−Zn(1)−S(2)	84.58(6)	83.48(6)	83.07(7)
N(1)−Zn(1)−O(2)_2		94.61(8)	

complex will not be discussed.[13] A structural drawing of the complex is available in the Supporting Information as Figure S1. Three complexes (**3**, **5**, and **6**) of the aryloxide family were characterized by X-ray crystallography. Details of the data collection and structure refinement for these complexes are given in Table 1. Selected bond distances and angles are given in Table 2. Structural drawings are shown in Figures 1 and 2.

In each zinc aryloxide structure, two nitrogen and two sulfur donors from the bmnpa or benpa chelate ligand are coordinated to the Zn(II) center. In **3** and **6**, the aryloxide ligand occupies a fifth coordination site, yielding a distorted trigonal bipyramidal geometry (**3**, $\tau = 0.80$; **6**, $\tau = 0.76$)[20]

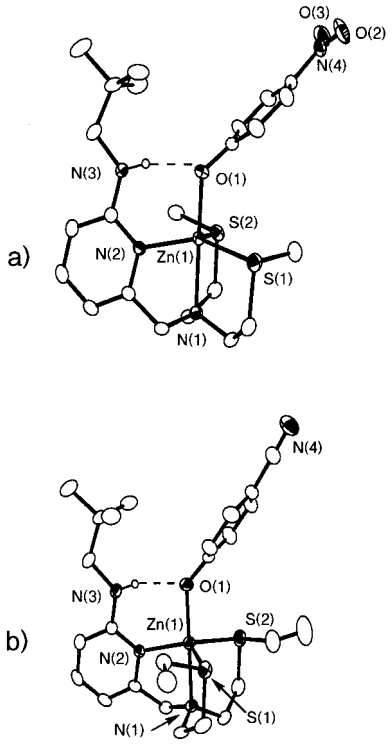

Figure 1. ORTEP representation of the cationic portions of (a) [(bmnpa)-Zn($OC_6H_4NO_2$)]ClO_4 (**3**) and (b) [(benpa)Zn(OC_6H_4CN)]ClO_4 (**6**). All ellipsoids are shown at the 35% probability level (all hydrogen atoms except the secondary amine hydrogen not shown for clarity).

for the cationic zinc center in each of these complexes. As with other monomeric five-coordinate metal complexes of the bmnpa ligand, two distinct N(py)−Zn−S(thioether) angles are observed in **3** and **6** (**3**, N(2)−Zn(1)−S(1)

(20) Addison, A. W.; Rao, T. N.; Reedijk, J.; von Rijn, J.; Verschoor, G. C. *J. Chem. Soc., Dalton Trans.* **1984**, 1349−1356.

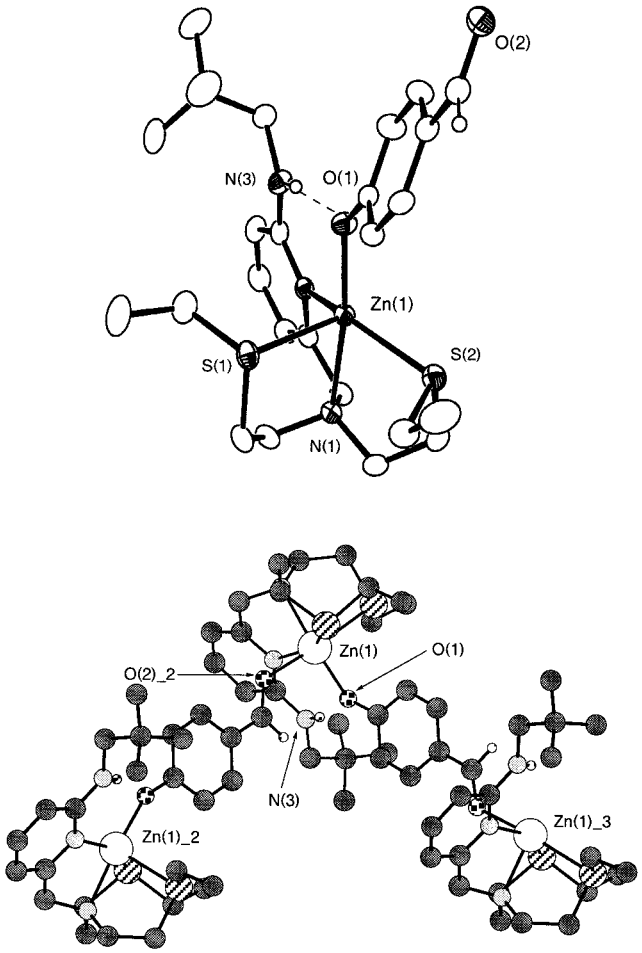

Figure 2. ORTEP representation of the coordination sphere of a single zinc center (top) in the solid state chain structure (Chem3D representation) of [(benpa)Zn(*p*-OC_6H_4CHO)]ClO_4 (**5**) (bottom). The bridging aryloxide groups that would extend the chain structure (bottom) from Zn(1)_2 and Zn(1)_3 are omitted for clarity. All ellipsoids are shown at the 35% probability level (all hydrogen atoms except the secondary amine and aldehyde hydrogen not shown for clarity).

130.54(7)°, N(2)−Zn(1)−S(2), 111.30(7)°; **6**, N(2)−Zn(1)−S(1) 116.29(7)°, N(2)−Zn(1)−S(2), 130.15(7)°). Notably, in both **3** and **6**, the larger N(2)−Zn(1)−S angle does not correspond to the location wherein the *S*-alkyl (Me or Et) substituent is located. This positioning of the thioether alkyl substituent in the area defined by the more acute N(2)−Zn(1)−S angle of the equatorial plane is also observed in [(bmnpa)Zn(ClO_4)](ClO_4).[13] In each of these complexes, the overall result of the difference in N(2)−Zn−S angles and direction of thioether alkyl substituent canting is the generation of a potentially available sixth coordination position in the equatorial plane. In **5**, this coordination site is filled by the aldehyde carbonyl oxygen of an aryloxide bound to another zinc cation, resulting in an overall distorted octahedral geometry for each Zn(II) ion and a chain-type structure. The observed N(2)−Zn(1)−S angles in **5** reflect the change in the metal ion geometry with a notable enlargement in one N(2)−Zn(1)−S bond angle (N(2)−Zn(1)−S(2), 150.05(6)°) and contraction in the other (N(2)−Zn(1)−S(1), 103.20(8)°). The angles of the equatorial plane involving the aldehyde carbonyl oxygen donor are acute (O(2)_Z−Zn(1)−N(2), 81.91(8)°; O(2)_Z−Zn(1)−S(2), 75.12(5)°).

Table 3. Distances (Å) and Angles (deg) of Hydrogen-Bonding Interactions in **3**, **5**, and **6**

	3	**5**	**6**
N(3)···O(1)	2.775(3)	2.776(3)	2.777(4)
N(3)−H···O(1)	160(3)	166(3)	162(3)

Despite their differences in overall coordination number, similar Zn−O(aryloxide) bond distances are observed for **3**, **6** (av 1.946(2) Å) and **5** (1.962(2) Å). These distances only slightly exceed those found in four-coordinate Zn−aryloxide complexes (1.86−1.91 Å).[11] The Zn−O(aldehyde) bond length found in **5** (2.228(2) Å) is >0.10 Å longer than those found in the octahedral [$Zn(BA)_4(ClO_4)_2$] (av 2.06 Å), [$Zn(BA)_5(H_2O)](BF_4)_2$ (av 2.09 Å), and [$Zn(BA)_2(CH_3CN)_4](BF_4)_2$ (av 2.12 Å) complexes (BA = benzaldehyde).[21] In these complexes, reported by Vahrenkamp et al., the Zn−O(aldehyde) bond distances were influenced by the nature of the coligands on the zinc center, with the longest Zn−O(aldehyde) bonds being found when the remaining coordination sites were occupied with increasing numbers of water and acetonitrile ligands. The long Zn−O(aldehyde) bond length in **5** (2.228(2) Å) is likely a consequence of the presence of two sulfur donors in the equatorial plane, as well as the weak donor properties of the aldehyde carbonyl group.

Consistent with the overall increase in coordination number of **5**, the Zn−S and Zn−N(py) distances of the equatorial plane are elongated in **5** as compared to those found for **3** and **6**. Specifically, whereas the average Zn−S distance in **3** and **6** is 2.466 Å, in **5** the average Zn−S distance is 2.578 Å.

An important biomimetic feature of complexes **4**−**10** is the presence of a single internal hydrogen bond donor in the bmnpa/benpa supporting ligand systems (Table 3). In complexes **3**, **5**, and **6**, a similar hydrogen-bonding interaction, involving the donor N(3)−H and the acceptor O(1) oxygen atom of the coordinated aryloxide ligand, is observed for each complex. In general, these hydrogen-bonding interactions are characterized by a N(3)···O(1) distance of ∼2.78(1) Å and a N(3)−H(3)···O(1) angle of ∼163(3)°. These parameters are consistent with the classification of these interactions as moderate hydrogen bonds.[6] Comparison of the hydrogen-bonding parameters found in these synthetic complexes with those found in inhibitor-bound forms of LADH (Table 4) indicates that the hydrogen-bonding interactions in **4**−**10** are characterized by a heteroatom distance that is generally similar to those found in the biological system (typically ∼2.6 Å), when the resolution of the protein crystal structures (1.8−2.5 Å) is taken into consideration. We also note that the hydrogen-bonding heteroatom distances found in **3**, **5**, and **6** are the shortest found thus far for zinc complexes of the bmnpa and related ligands.[13,15] This is consistent with the greater negative charge on the aryloxide oxygen in these complexes, as compared to a neutral carbonyl oxygen donor (e.g., *N*,*N*-DMF),[15] making the former a better hydrogen bond acceptor.

FTIR Spectroscopy. Solid state and solution FTIR studies of the zinc aryloxide complexes were undertaken in order

(21) Müller, B.; Vahrenkamp, H. *Eur. J. Inorg. Chem.* **1999**, 117−127.

Table 4. Comparison of Hydrogen-Bonding Interactions with LADH

	heteroatoms	distance (Å)
[(bmnpa)Zn($OC_6H_4NO_2$)]ClO_4 (**3**)	N(3)···O(1)	2.775(3)
[(bmnpa)Zn(OC_4H_4CHO)]ClO_4 (**5**)	N(3)···O(1)	2.776(3)
[(bmnpa)Zn(OC_6H_4CN)]ClO_4 (**6**)	N(3)···O(1)	2.777(4)
[(bmnpa)Zn($OClO_3$)]ClO_4	N(3)···O(1)	2.93[a]
[(bmapa)Zn(*N*,*N*-DMF)]$(ClO_4)_2$	N(1)···O(1)	2.86[b]
LADH (alkoxide: calcd)	O(Ser_{48})···O(alkoxide)	2.44[c]
LADH (DMSO inhibited; 1.8 Å)	O(Ser_{48})···O(DMSO)	2.6[d]
LADH (*N*-CyForm inhibited; 2.5 Å)	O(Ser_{48})···O(*N*-CyForm)	2.6[e]
LADH (*N*-FormPip inhibited; 2.5 Å)	O(Ser_{48})···O(*N*-FormPip)	2.5[e]

[a] Berreau, L. M.; Allred, R. A.; Makowska-Grzyska, M. M.; Arif, A. M. *Chem. Commun.* **2000**, 1423−1424. [b] bmapa = *N*,*N*-bis-2-(methylthio)-ethyl-*N*-(6-amino-2-pyridylmethyl)amine: Berreau, L. M.; Makowska-Grzyska, M. M.; Arif, A. M. *Inorg. Chem.* **2001**, *40*, 2212−2213. [c] Agarwal, P. K.; Webb, S. P.; Hammes-Schiffer, S. *J. Am. Chem. Soc.* **2000**, *122*, 4803−4812. [d] Al-Karadaghi, S.; Cedergren-Zeppezauer, E.; Hövmoller, S.; Petratos, K.; Terry, H.; Wilson, K. S. *Acta Crystallogr.* **1994**, *D50*, 793−807. [e] *N*-CyForm = *N*-cyclohexylformamide; *N*-FormPip = *N*-formylpiperidine: Ramaswamy, S.; Scholze, M.; Plapp, B. V. *Biochemistry* **1997**, *36*, 3522−3527.

to correlate their X-ray crystallographically determined structures with their solution behavior and to more fully understand the hydrogen-bonding interaction involving the zinc-bound aryloxide oxygen atom and zinc−carbonyl oxygen interactions in **5**. For each aryloxide complex, the N−H stretching vibration is broadened and shifted to lower energy as compared to the free ligand, consistent with its involvement in a hydrogen-bonding interaction in the solid state in **3**−**10**. Notably, in complex **5**, the N−H stretching vibration (3254 cm^{-1}) is found ∼38 cm^{-1} higher than that observed for **3**, **4**, **6**, and **8**−**10** (av 3216 cm^{-1}). The shift to higher energy in **5** is likely due to electronic perturbation of the aryl ring induced by coordination of the carbonyl oxygen to a second zinc center, as is observed in the solid state structure of **5**. This coordination will withdraw electron density from the ring, making the aryloxide oxygen less electron rich and therefore a poorer hydrogen bond acceptor. The net result is an N−H bond strength in **5** that is closer to that of the free ligand (3400 cm^{-1}) than that of the zinc aryloxide derivatives wherein coordination to a second zinc center does not occur.

Solid state FTIR spectra of *p*-hydroxybenzaldehyde indicate a $\nu_{C=O}$ at 1666 cm^{-1}. As the region of 2000−1625 cm^{-1} in solid state FTIR spectra of **5** does not contain any vibrations of even weak intensity, a carbonyl stretching vibration ($\nu_{C=O}$) could not be readily identified for this complex. This indicates that $\nu_{C=O}$ in **5** is likely shifted to lower energy and located beneath another medium/strong vibration associated with the pyridine ring of the ligand in the region of 1600−1630 cm^{-1}. In CH_2Cl_2 (∼100 mM), **5** exhibits a $\nu_{C=O}$ vibration at 1685 cm^{-1} whereas the carbonyl stretching vibration for free *p*-hydroxybenzaldehyde is found at 1689 cm^{-1}. Generally similar results are obtained in CH_3CN solution ($\nu_{C=O}$: **5**, 1680 cm^{-1}; *p*-hydroxylbenzaldehyde, 1690 cm^{-1}). This indicates that the chain-type structure observed in the solid state for **5** likely breaks apart in CH_2Cl_2 and CH_3CN solution via cleavage of the intermolecular Zn−O(aldehyde) interactions.

Solid state FTIR spectra of **7** exhibit a $\nu_{C=O}$ stretching vibration shifted to lower energy (1648 cm^{-1}) as compared to its position in solid state spectra of *p*-hydroxyacetophenone (1663 cm^{-1}). While this shift (15 cm^{-1}) may indicate zinc coordination of the ketone carbonyl oxygen in the solid state, we speculate that it may be due instead to a decrease in the electronic density of the aryloxide moiety as a whole, resulting from zinc complexation of the deprotonated aryloxide oxygen atom.[22] We have developed this hypothesis based on the results of solution FTIR studies of **7** in solvents of differing donor properties. Specifically, in CH_2Cl_2 or CH_3CN solution (∼100 mM), the $\nu_{C=O}$ vibration for **7** is found at 1662 cm^{-1}, still ∼13−14 cm^{-1} lower than that observed for free *p*-hydroxyacetophenone under identical conditions (∼100 mM CH_2Cl_2 solution, 1675 cm^{-1}; ∼100 mM CH_3CN solution, 1676 cm^{-1}). As CH_3CN may be anticipated to be a better donor for the zinc cation than would be the ketone carbonyl oxygen atom, it is unlikely that the shift observed in both CH_2Cl_2 and CH_3CN solution arises from a Zn−carbonyl oxygen interaction. At this point, it is important to distinguish the fact that this is not the case for the aldehyde-appended aryloxide derivative **5**, wherein the difference in $\nu_{C=O}$ between **5** and *p*-hydroxybenzaldehyde in solid state spectra is >40 cm^{-1}. In solution spectra in CH_2Cl_2 or CH_3CN, this difference drops to 5 and 10 cm^{-1}, respectively, indicating a more significant perturbation of the carbonyl moiety of **5** in the solid state.

The aryl carbon−O(1) stretching vibration (ν_{C-O}) in complexes **3**−**10** is found in the region of 1260−1305 cm^{-1}, with those possessing a para-electron-withdrawing group found at ≈1279 cm^{-1} (**3**−**8**) and the complex which possesses a para-electron-donating group (**10**) at 1261 cm^{-1}.

^{1}H and ^{13}C NMR. The ^{1}H NMR spectroscopic features (Table S3) of **4**−**10** are similar, indicating that the solution structures of these complexes are quite comparable. For example, **4** exhibits ^{1}H NMR spectral features in CD_3CN solution that are generally similar to those observed for **5**. Coupled with the solution FTIR studies of **5** in CH_3CN solution (vide supra), this indicates that the chain structure observed in the solid state for **5** is cleaved in CH_3CN solution. With the exception of the chemical shift of the secondary amine proton, the chemical shifts of the aryl and alkyl protons of the benpa ligand vary only slightly in **4**−**10**. For example, the singlet resonance observed for the benzylic protons in **4**−**10** is found at 3.87 ± 0.04 ppm.

The chemical shift of the secondary amine proton (N(3)−*H*) in **3**−**10** can be correlated with the pK_a of the parent phenol (Figure 3). This is exemplified by comparing the chemical shift of the N−*H* proton for **4** (8.93 ppm; pK_a *p*-nitrophenol = 7.14) with that of **10** (9.97 ppm; pK_a *p*-methoxyphenol = 10.2). The downfield shift of the N(3)−*H* resonance in **10** indicates that a stronger hydrogen-bonding interaction is present in this complex, resulting from the increased basicity of the aryloxide moiety.[6]

(22) (a) Müller, B.; Vahrenkamp, H. *Eur. J. Inorg. Chem.* **1999**, 129−135. (b) Müller, B.; Vahrenkamp, H. *Eur. J. Inorg. Chem.* **1999**, 137−144.

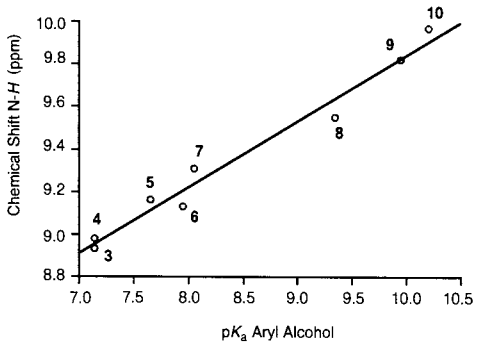

Figure 3. Correlation of chemical shift of N(3)−*H* proton resonance of **3**−**10** (dry CD_3CN solution, 20(1) °C) with pK_a of parent aryl alcohol.

The ^{13}C NMR data (Table S4) of **3**−**10** display substantial variability only in the chemical shift of the carbons of their respective aryloxide ring. The carbonyl carbon ^{13}C resonances for **5** and **7** are found at 191.3 and 197.1 ppm, respectively. These chemical shifts are very similar to those found in the free aryl alcohols (192.1 and 197.8 ppm, respectively), indicating little perturbation of the electron density in the carbonyl unit for the zinc-bound aryloxide in CD_3CN solution. This result further suggests that the aldehyde oxygen in **5** is not retained as a zinc ligand in CD_3CN solution.

Discussion

Preparation of synthetic complexes relevant to species proposed to occur in the catalytic cycle of LADH has been the goal of a number of previous synthetic investigations.[7,8c,10b,11,12] Of particular interest has been the generation of mononuclear zinc complexes possessing a single deprotonated alcohol ligand, species relevant to the proposed active form of LADH. Notably, previous studies by Vahrenkamp et al. yielded structurally characterized examples of tetrahedral nitrogen-ligated zinc aryloxide complexes.[11b] These complexes, which possess a supporting tris(pyrazolyl)hydroborato ligand, were generated upon reaction of a zinc hydroxide precursor ($Tp^{Cum,Me}Zn-OH$, $Tp^{Ph,Me}Zn-OH$, or $Tp^{tBu,Me}Zn-OH$) with the appropriate aryl alcohol (phenol, *p*-nitrophenol, 2-hydroxy-3-methoxybenzaldehyde (*o*-vanillin), 2-hydroxybenzyl alcohol (salicylic alcohol), 2,6-bis(hydroxymethyl)-*p*-cresol).[11b] In all cases, the $Tp^{R,R}Zn-OAr$ derivatives were prepared under stoichiometric reaction conditions in yields >50%, albeit those prepared from the most acidic alcohol (*p*-nitrophenol) were isolated in the highest yields (83−89%). A structurally related family of mononuclear zinc aryloxide complexes of the general formula $Tp^{tBu,Me}Zn-(p\text{-}OC_6H_4X)$ (X = NO_2, $C(O)CH_3$, $C(O)OCH_3$, I, H, CH_3, tBu, OCH_3) has been reported by Parkin et al.[11e] In this case, all of the aryloxide derivatives were prepared from reaction of a zinc hydride precursor ($Tp^{tBu,Me}Zn-H$) and the appropriate aryl alcohol. This was necessary because the aryloxide complexes ($Tp^{tBu,Me}Zn-(p\text{-}OC_6H_4X)$ are thermodynamically unstable with respect to hydrolysis, forming equilibrium mixtures with the hydroxide derivative $Tp^{tBu,Me}Zn-OH$ and free aryl alcohol in the presence of water. Determination of the equilibrium constants of these hydrolysis reactions at 300 K revealed that formation of a zinc aryloxide derivative was favored by incorporation of a para-electron-withdrawing substituent on the aromatic ring.

Additional research by Parkin et al. revealed that mononuclear alkoxide complexes of the general formula $Tp^{tBu,Me}Zn-OR$ are also thermodynamically unstable with respect to hydrolysis, forming equilibrium mixtures in the presence of water that lie significantly toward the hydroxide derivative ($Tp^{tBu,Me}Zn-OH$).[11e] On the basis of these results, the zinc alkoxide intermediate that is proposed to form during the catalytic cycle of LADH would be expected to be very unstable with respect to hydrolysis, unless structural or electronic features (e.g., hydrogen-bonding involving Ser_{48}, a mixed nitrogen/sulfur ligand environment) within the active site of the enzyme in some way promote alkoxide formation.

The family of zinc aryloxide complexes reported herein was prepared in order to initiate investigations into how properties of the active site of LADH influence the chemistry of a zinc-bound deprotonated alcohol ligand. In particular, we are interested in the effect of hydrogen-bonding on the thermodynamic stability of zinc alkoxide species with respect to hydrolysis. As described herein, synthesis of this family of nitrogen/sulfur-ligated zinc aryloxide complexes was achieved starting from the zinc hydroxide precursors $[(bmnpaZn)_2(\mu\text{-}OH)_2](ClO_4)_2$ or $[(benpaZn)_2(\mu\text{-}OH)_2](ClO_4)_2$. Use of excess molar equivalents of the respective aryl alcohol was necessary in order to avoid isolation of mixtures of the desired aryloxide complex and its hydroxide precursor, suggesting that equilibria involving the water produced in the reaction are likely present in these systems. Future work will be directed at delineating how the presence of a single internal hydrogen bond donor, the mixed N/S-coordination environment, and the electronic properties of the zinc-bound aryloxide influence zinc hydroxide/aryloxide equilibria. That being said, an approach currently being pursued in our laboratory toward examining the effect of a single hydrogen-bonding interaction on the chemistry of N/S-ligated zinc aryloxide species involves the construction and examination of the hydrolytic properties of an analogous family of zinc aryloxide complexes supported by the structurally related *N*,*N*-bis-2-(methylthio)ethyl-*N*-(2-pyridylmethyl)amine (bmpa) ligand.[23]

An important component of accurate model systems for the active site zinc ion in LADH is the use of ligands that provide a mixed nitrogen/sulfur coordination environment, preferably involving thiolate donors in order to mimic the electronic character of coordinated cysteine residues. Ideally, these complexes would also demonstrate reactivity properties pertinent to the enzyme. The ligands employed herein provide an N_2S_2 coordination environment involving thioether sulfur donors. While the presence of neutral thioether sulfur donors in these complexes may be anticipated to produce a zinc center that is more Lewis acidic than the active site zinc ion in LADH, this may be tempered to some degree by the presence of an additional nitrogen donor. Therefore, while

(23) Ambundo, E. A.; Deydier, M.-V.; Grall, A. J.; Aguera-Vega, N.; Dressel, L. T.; Cooper, T. H.; Heeg, M. J. Orchrymowicz, L. A.; Rorabacher, D. B. *Inorg. Chem.* **1999**, *38*, 4233−4242.

these complexes are not perfect structural models for the proposed active species formed in the catalytic cycle of LADH, they will enable the first opportunity to systematically examine the hydrolytic reactivity of nitrogen/sulfur-ligated zinc aryloxide species possessing a single internal hydrogen bond donor. Efforts are also underway to modify the ligand systems utilized herein to include thiolate donors, so as to be able to directly examine the chemical effect of neutral versus anionic sulfur ligation. In this regard, to our knowledge, only one thiolate-ligated zinc aryloxide complex has been previously reported ([Zn(L3S)(OPh^{p-NO2})], where L3S = bis(3,5-dimethylpyrazolyl)(1-methyl-1-sulfanylethyl)-methane), albeit its solid state structure was not elucidated by X-ray crystallography.[11f]

The preparation and characterization of this particular family of zinc aryloxide complexes has enabled an initial evaluation of how a single hydrogen-bonding interaction involving a zinc-bound deprotonated alcohol ligand is perturbed upon changes in the basicity of the alcoholate moiety. As outlined in Figure 3, we have discovered that deshielding of the N−*H* resonance in these complexes can be correlated with increasing pK_a of the parent aryl alcohol. This result suggests that the hydrogen-bonding interaction involving the zinc-bound aryloxide ligand is becoming stronger as the aryloxide fragment increases in basicity.[6] While the structurally characterized aryloxide complexes reported herein do not reveal differences in hydrogen-bonding heteroatom distances, it must be noted that **3**, **5**, and **6** are derived from aryl alcohols found in a very narrow pK_a range (7.15−7.95, as measured in water). Therefore, an important future goal is structural characterization of zinc aryloxide complexes derived from higher pK_a aryl alcohols and, more importantly, zinc alkoxide derivatives. In regard to LADH, these results suggest that the strength of the hydrogen-bonding interaction between Ser_{48} and a zinc-bound alkoxide may be modulated by changes in the basicity of the alkoxide.

Concluding Remarks

The mononuclear zinc aryloxide complexes reported herein demonstrate the feasibility of the bmnpa/benpa ligand frameworks for supporting nitrogen/sulfur-ligated zinc complexes possessing a single deprotonated alcohol ligand. These complexes are relevant to the proposed active form of LADH. The inclusion of a single internal hydrogen bond donor in **3**−**10** mimics the proposed active site secondary hydrogen-bonding interaction involving Ser_{48} and a zinc-bound alkoxide in the enzyme. As suggested by Plapp[2] and Hammes-Schiffer,[3] and reiterated by Parkin,[11e] hydrogen bonding may play a key role in stabilization of the zinc alkoxide intermediate in LADH. That being said, this work provides the foundation for future reactivity studies directed at elucidating the effect of hydrogen-bonding on the chemistry of nitrogen/sulfur-ligated zinc aryloxide species.

Acknowledgment. We acknowledge the support of the donors of the Petroleum Research Fund (ACS-PRF 36394-G3), administered by the American Chemical Society, and the National Science Foundation (CAREER Award CHE-0094066). We also thank Magdalena M. Makowska-Grzyska for technical assistance and valuable discussions and the reviewers for helpful comments.

Supporting Information Available: X-ray crystallographic files, in CIF format, for the structure determinations of **2**, **3**, **5** and **6**. An ORTEP diagram (Figure S1) of the cationic portion of [(benpaZn)$_2$(μ-OH)$_2$](ClO_4)$_2$ (**2**) and tables outlining the details of X-ray data collection and refinement for **2** (Table S1) and comparison of bond distances and angles between [(bmnpaZn)$_2$-(μ-OH)$_2$](ClO_4)$_2$ (**1**) and **2** (Table S2). Tables of ^{1}H and ^{13}C NMR data (Tables S3 and S4) for complexes **1**−**10**. This material is available free of charge via the Internet at http://pubs.acs.org.

IC020031Q